Walls in liquid crystalline polymers: an electron microscopy study

A. M. Donald* and A. H. Windle
Department of Metallurgy and Materials Science, Pembroke Street, Cambridge CB2 3QZ, UK
(Received 12 December 1983)

Walls between domains in an annealed liquid crystal polymer are examined in the transmission electron microscope. The associated contrast in bright field and for various positions of aperture in dark field has been interpreted in terms of the chain reorientation routes across the walls. In addition, the possible wall orientations for a given pair of adjacent domains have been analysed in the light of the necessity of constant chain flux normal to the wall. This condition is also shown to limit the available reorientation routes and simplify the experimental determination of wall structure. Specimens of a thermotropic copolyester annealed for 5 s at 300°C show walls which tend to lie parallel to the original shear direction. The chain orientation in the wall is locally more closely confined to the specimen plane than in the domains, and the distortion type is twist. After longer anneals the walls change contrast in bright field and appear as dark veins. Detailed analysis of micrographs obtained under different imaging conditions shows that the change in character of the walls is associated with a change in reorientation route. The chain axes within the walls that appear as dark veins rotate through the orientation where they are nearly perpendicular to the specimen plane. The stereographic projection is used throughout to illustrate the orientation relationships between the adjacent domains, the chain axes within the wall and the orientation of the wall itself.

(Keywords: liquid crystalline polymers; mesophase; copolyester; disclination wall; electromicroscopy; domain)

INTRODUCTION

The concept of 'domains' separated by 'walls' of various types, is well documented for small molecule liquid crystals (SMLC's)[1-5]. The possible orientations of the molecules are strongly controlled by the interaction of the molecules with the constraining surfaces, and in general, domains will occur whenever energetically equivalent but orientationally different configurations can arise.

The recent synthesis of a new group of liquid crystals, thermotropic liquid crystalline polymers (LCP's), has raised new questions concerning the available low energy configurations when few chain ends are present. As has been discussed by Meyer[6], severe restrictions are imposed for the limiting case of infinite molecular weight, namely that only homogeneous planar) textures are permitted in which the molecular orientation always lies parallel to the constraining surfaces, because any alignment with a perpendicular component requires the condensation of chain ends at the surface. Furthermore, two dimensional splay distortions cannot occur, since these also involve the presence of chain ends[7].

Polarized light microscopy is the technique normally used to investigate domain and wall structures in SMLC's[3,8-10]. The successful application of transmission electron microscopy (*TEM*) to orientation analysis of LCP's has recently been demonstrated[11,12]. *TEM* cannot be easily used for SMLC's, but the possibility of quenching mesophase structures of LCP's into the solid state at room temperature[13] permits its use on these systems. The technique has two major advantages over optical microscopy: firstly it possesses much higher resolution (even for LCP's for which radiation damage limits the magnification that can be used) and secondly, direct correlation of orientation information obtained from a diffraction pattern with the microstructural information of the image can be made. This second point is particularly useful for LCP's, where the identity of the molecular long axis and the local extinction axis for polarized light cannot be assumed[14].

From optical microscopy and *TEM* studies it has been possible to show that upon shearing, thermotropic melts of a range of random copolyester LCP's develop a characteristic banded microstructure, in which the molecules follow a serpentine path about the shear axis[11,15,16]. This structure is predominantly planar, i.e. the variation in the molecular orientation out of the plane of the specimen is thought to be smaller than that within the plane[12]. When thin films containing the banded structure are annealed on a rocksalt substrate, a significant rearrangement occurs to give a structure in which domains of constant orientation are elongated along the shear direction. This structure is in contrast to the original banded texture in which the orientation is correlated along lines perpendicular to the shear direction.

Recent *TEM* studies[12] have shown that, simultaneously with the rearrangement of the molecules into domains on annealing, an out-of-the-plane component of molecular tilt develops which can give contrast in bright field. It appears that alternate domains adopt 'up' and 'down' tilts, so that on tilting the specimen in the microscope about an axis perpendicular to the shear

* Present address: Cavendish Laboratory, Madingley Road, Cambridge, UK.

0032-3861/84/091235-12$03.00

direction, the inclination of the molecules to the electron beam is increased in one set of domains and decreased in the other. As the molecular axis approaches the beam direction, the extent of the equatorial ring which is significantly excited increases, leading to a decrease in the intensity of the unscattered beam. Hence, domains with a small inclination of the molecules to the beam appear dark in the bright field image relative to the domains in which the molecules are nearly perpendicular. Upon reversing the sense of tilt, the contrast between the domains is also reversed.

Clearly a region of orientational transition between adjacent domains must occur. In specimens of one particular copolyester annealed for 10 min or longer on rocksalt, prominent dark 'veins' develop in the bright field image, and these tend to lie parallel to the prior shear direction[11,16]. The veins correspond to regions in which the tendency towards homeotropy is most fully developed, and hence they appear blackest in bright field images of untilted films. In this paper a more detailed analysis of the molecular configurations within the veins will be presented, together with a discussion of other boundaries that may be present but are not apparent from bright field microscopy alone.

WALL TYPES IN SMALL MOLECULE LIQUID CRYSTALS

For SMLC's the occurrence of walls seems to be relatively rare, since for typical anchoring energies, W_s, and film thicknesses t, it can be shown that it is energetically favourable for the wall to split into two surface lines if

$$t \gtrsim \frac{2K}{W_s}$$

where K is a Frank elastic constant (see e.g. refs. 3 and 5). Walls have been observed for systems where W_s is abnormally low, as in Ryschenkow's anchoring. Two general types of walls can be identified which, by analogy with walls separating domains of opposite magnetization in ferromagnetic materials, may be designated as Neel and Bloch types. An alternative classification for such walls terms them inversion walls of the first and second kind respectively[2], and in addition, Bloch walls are sometimes known as 'tilt inversion walls'[4].

Whereas, both for Bloch walls in ferromagnets and for inversion walls in liquid crystals as originally envisaged by Nehring and Saupe[2], a rotation of π is assumed, Ryschenkow and Kleman[3] implicitly recognize that walls may exist between domains with a misorientation of less than π. An analysis of the types of elastic distortions necessarily associated with the two types of walls shows that a Bloch wall may be achieved via twist distortions alone (although other distortions may also occur), but Neel walls must involve both bend and splay, although not twist. For SMLC's in general, twist is known to be the smallest energy distortion (e.g. ref. 17), but Bloch walls may not be favoured if there is preferential alignment of the molecules parallel to the constraining surfaces, as is often the case.

POSSIBLE WALL GEOMETRIES IN LCP's

Compared with small molecule liquid crystals, a polymeric material will have a comparative dearth of chain ends. If the possibility of segregation of those chain ends which are present into planar regions is discounted for the moment, then the requirement of continuity across a wall means that the flux of molecules must be the same on both sides. As a consequence, the wall must contain one of the two angular bisectors of the two domain orientations. This condition does not define the wall orientation uniquely for any given pair of orientations, but it does restrict the number of possibilities.

Figure 1a shows two domain orientations D_1 and D_2, plotted as poles on a stereographic projection (the open circles mark the opposite poles on the bottom hemisphere). Although the poles are plotted equidistant from the centre of the stereogram, they are in a general orientation with respect to each other. The crosses, B_1 and B_2, mark the orientations of the two bisectors (and their antipoles) which are contained in the common plane

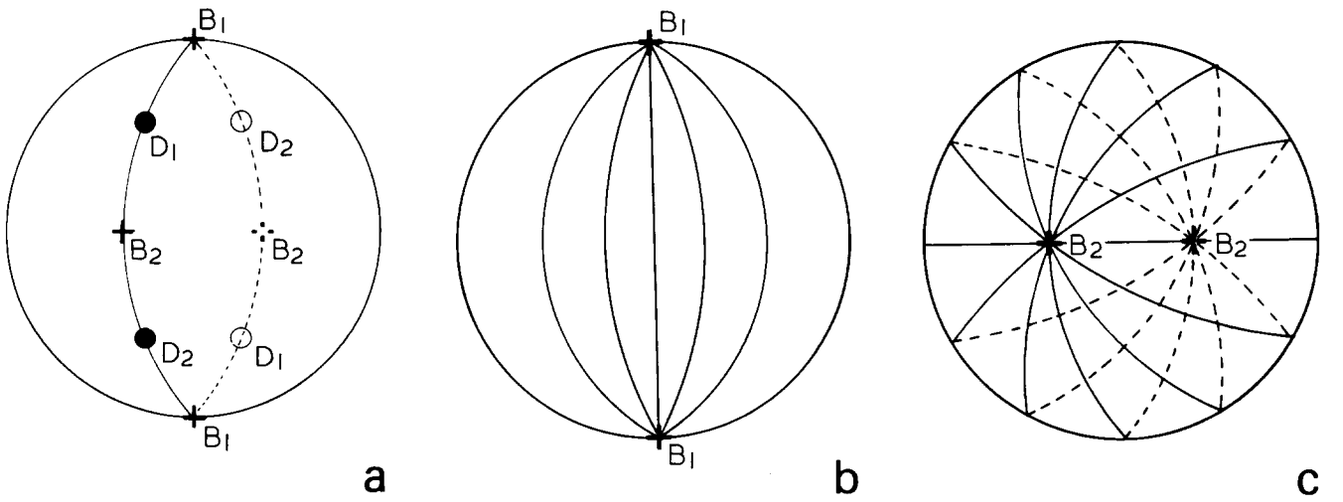

Figure 1 (a) Stereographic projection of typical molecular orientations in two adjacent domains, plotted as poles D_1 and D_2, and the corresponding bisectors of the angles between these orientations, plotted as B_1 and B_2. The great circle represents the plane containing the orientations D_1 and D_2. (b) Great circle plots of possible wall orientations which contain the orientation of the bisector B_1. (c) Examples of possible wall orientations passing through the bisector B_2

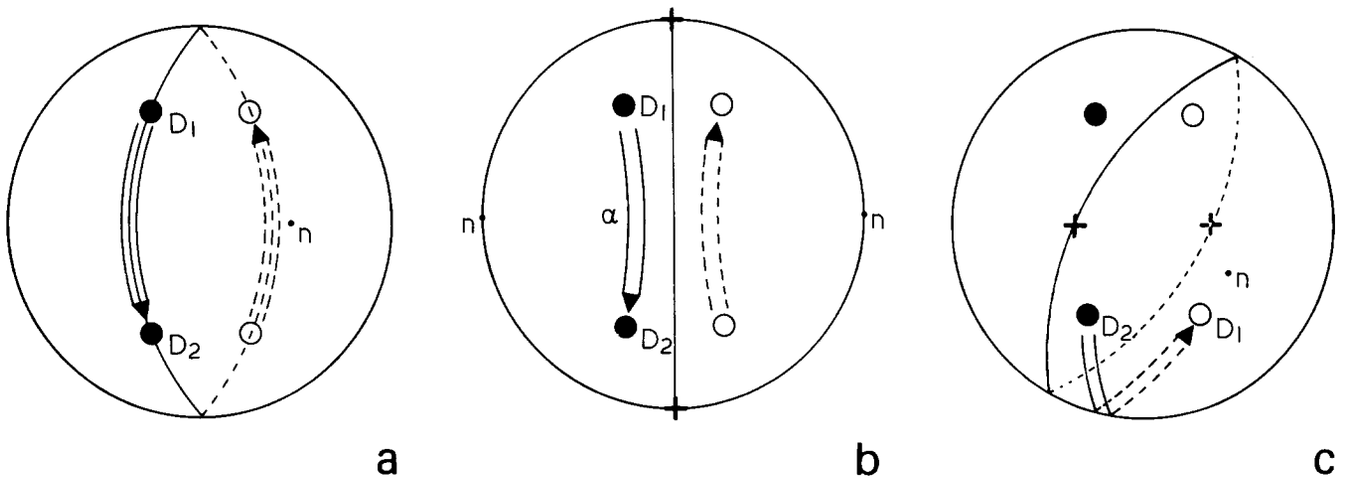

Figure 2 (a) Stereogram of a wall orientation (great circle) which contains both D_1 and D_2. The route by which the chains reorient within the wall is marked by the double arrow and also lies within the plane of the wall. (b) Small circle reorientation route for a wall drawn through B_1 (see *Figure 1b*) and normal to the plane of the stereogram. Such a route is able to maintain constant chain flux within the plane of the wall. (c) Another example of a small circle reorientation route for a wall containing the bisector B_2 (*Figure 1c*)

containing D_1 and D_2 (the great circle). *Figures 1b* and *1c* show great circle traces representing the family of wall orientations which permit continuity of molecular flux. They pass through the respective directions B_1 and B_2. The second factor to consider is the molecular organization within the wall. Again, in the absence of chain ends, it will be energetically desirable for constant molecular flux not only to be equal in the two domains, but to remain constant at all points through the thickness of the wall itself. It is thus necessary for the angle between the local molecular orientation within the wall and the normal to the wall to remain constant; this requires that the local molecular orientation reorients by rotation around a cone, which has the wall normal as its axis.

Figure 2a shows the special case in which the plane of the wall contains both domain orientations as well as their bisectors. The reorientation path is contained within the plane of the wall, as marked by the double arrow. For this case, which is a great circle route, the distortion in the wall is pure twist. Since the molecules possess no sense of polarity (opposite ends indistinguishable), either the rotation + or − may occur, but energetically the shorter reorientation path may be expected. For the more general case, where the two domain orientations are not contained in the plane of the wall, the local orientation within the wall rotates on a small circle which represents the cone, so as to maintain a constant angle with the wall normal. Two examples are illustrated in *Figures 2b* and *2c*. In each case the requirement of constant flux means that the wall contains a bisector of the angle between the two domain orientations (marked as +) and the reorientation routes, a 'short route', α, and its complementary but longer route $\pi-\alpha$ (not traced), lie on small circles which have the normal to the wall as their angular centres.

From these diagrams it is clear that, in the absence of chain ends, one particular wall orientation exists for which only twist distortions are involved. However, there are also a range of other possible wall orientations for which combined twist and bend distortions occur. In ferromagnets, the necessity for the continuity of the normal component of magnetization at a wall, leads to the characteristic geometry of the Bloch wall. It seems that in LCP's, the constant flux requirements across a wall lead

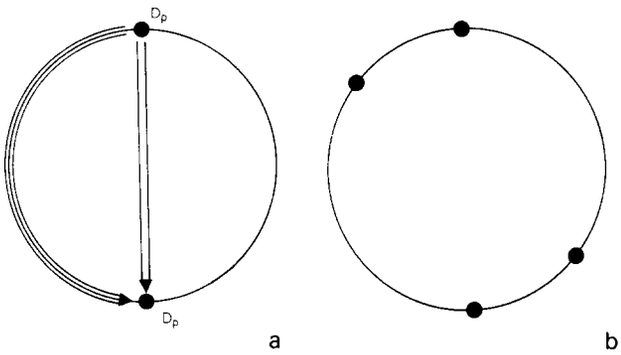

Figure 3 (a) Stereogram of two domain orientations, D_p, lying in the plane of the specimen. They are separated by π and thus indistinguishable for the molecules under consideration. Of the many possible wall orientations which contain D_p, only two are shown as indicated by reorientation arrows. (b) Poles for domain orientations in the specimen plane but with a general misorientation angle

to a close analogy with magnetic Bloch walls; for SMLC's, with the much greater availability of chain ends and the consequent possibilities of splay distortions, the similarity with magnetic materials may be much less close. However, for crystalline ferromagnets, it must be borne in mind that the geometry of magnetic walls is modified by the existence of crystallographically related easy directions of magnetization, for which no equivalent in LCP's can readily be identified.

The arguments presented so far have only considered bulk samples. If the specimen is thin in one direction, the existence of surfaces becomes important, and the intersection of the surface planes with the long molecules must be a significant factor. The density of chain ends required at the LCP surface will be dictated by the degree to which the molecules are tilted out of the plane, and the density will necessarily change at a wall with the associated rapid change in local tilt orientation. In cases where chain ends are unavailable or the molecules have been constrained to lie flat between glass slides or other surfaces, domain orientations will lie on the primitive of the stereogram, where this represents the plane of the specimen. *Figure 3a* shows two such domain orientations separated by π. It is apparent that in this particular

example, a range of twist walls (great circle routes) is possible. For a thin specimen, two limiting cases of wall orientations may be expected to be important: either the orientation will everywhere remain within the specimen plane, in which case the boundary will also lie in that plane, or the plane of the wall may lie normal to the specimen. This latter orientation will minimize the area of the walls, but simultaneously require a large density of chain ends at the surface in its immediate vicinity, as the local orientation within a wall passes through exact homeotropy (centre of the sterogram).

Because of the non-polarity of the molecules, *Figure 3a* represents a special, degenerate case. In the more general situation, where the two domain orientations are contained in the specimen plane but misoriented by some arbitrary angle as shown in *Figure 3b*, the only pure twist wall possible is the one parallel to the specimen plane. Furthermore, if the local molecular orientation is to remain in the specimen plane at all points within the wall, there is no other wall orientation for which constant molecular flux can be maintained. Hence, any wall normal to the specimen will locally require high energy splay distortions, and therefore may not be expected to occur. A wall perpendicular to the specimen plane is a direct analogy of a Neel wall in a thin magnetic specimen, where in order to avoid surface poles, the magnetization direction remains within the specimen plane, although at the cost of stray field energy at the wall.

EXPERIMENTAL

The LCP used in this study was a random copolyester based on hydroxybenzoic and hydroxy naphthoic acids and designated B–N:

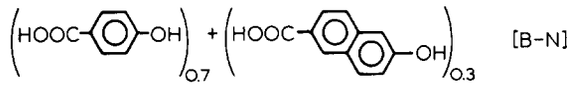

[*p*-hydroxybenzoic acid] + [hydroxynaphthalic acid]

Its intrinsic viscosity was 4.5, which is at the lower end of the range for similar materials previously examined[12]. To prepare thin films suitable for *TEM* the method detailed in ref. 12 was used. A small quantity of the polymer, held at 300°C, was sheared between a rocksalt substrate and a glass slide. The film was then annealed on the rocksalt for up to 10 min at 300°C, and quenched onto a metal block. Specimens were coated with carbon, and picked up on a copper grid from a distilled water bath after dissolution of the rocksalt. They were examined using a Philips 300 electron microscope operating at 100 KeV and fitted with a single tilt stage (±42°).

RESULTS

The diffraction pattern of unannealed specimens exhibiting the banded structure shows equatorial arcs. At longer annealing times the arcs increase in length and ultimately merge to form a full, although not completely uniform, ring[16,22]. For dark field microscopy it is possible to use a range of objective aperture positions in relation to the equatorial arcs. These positions together with the terminology used to identify them, are shown in *Figure 4*.

Figure 5 shows the domain microstructure developed from a banded structure by a short (5 s) anneal at 300°C. The bright field image (*Figure 5a*) shows diffraction contrast which renders the domain walls light. As already discussed[12] the molecules within the domains are tilted out of the specimen plane. The light contrast in the walls indicates that the molecules locally remain more parallel to the specimen plane. The corresponding dark field $E[W]$ image (*Figure 5b*) shows domain contrast representative of different molecular orientations.

It has already been established that the dark contrast walls which appear in bright field after longer anneals represent regions where the molecules are inclined steeply to the specimen plane[12,16]. The effect is most noticeable for specimens with a low average molecular weight and appears to be associated with segregation of the shorter chains to the walls. A bright field image showing the dark walls, or 'veins' is shown in *Figure 6a*. More information on the way the orientation varies across the domain wall can be obtained by considering the dark field images shown in *Figures 6b* and *6c*. Comparison of *Figures 6a* and *6b* show that the boundaries apparent in the bright field and interchain meridian dark field images correlate closely in both position and width (20–30 nm). The dark field image formed in one wing of the equatorial (E[W]), *Figure 6c*, shows several additional features: substantial contrast variations exist between domains separated by the walls visible in bright field images, but relatively sharp contrast changes also occur where no feature is visible in *Figure 6a*. Boundaries that do correlate with bright field features may appear as either light or dark lines in *Figure 6c*. The width of the light lines is comparable with *Figure 6a*, but the dark ones are much narrower. In *Figure 6c* an example of a change in contrast in the $E[W]$ dark field image which is not apparent in bright field is shown at A. Such contrast changes tend to occur along lines perpendicular to the shear direction. They are also clearly apparent in *Figure 7* which consists of bright field (a), IM[W] (b) and E[W] (c) images. Those walls per-

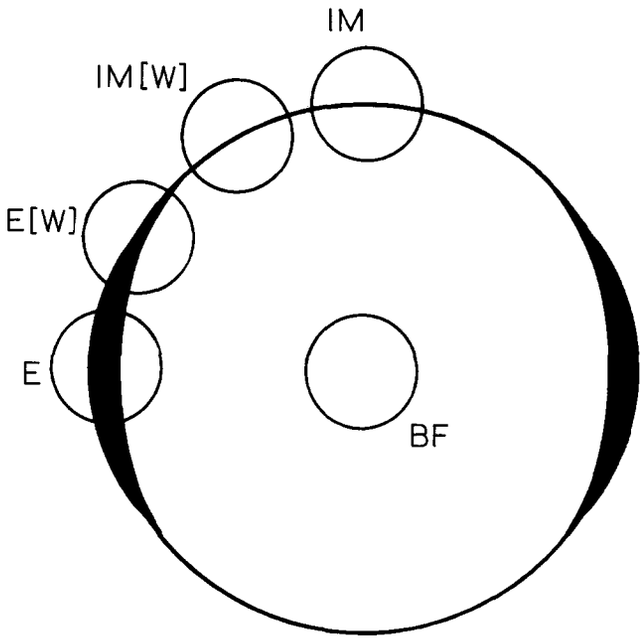

Figure 4 Schematic diagram showing different aperture positions with respect to a diffraction pattern with the shear direction vertical. E, centre of equatorial maximum; E[W], wing of equatorial; IM, interchain meridian, i.e., aperture positioned on meridian but at the same radius as the equatorial maximum; IM[W], wing of interchain meridian; BF, bright field

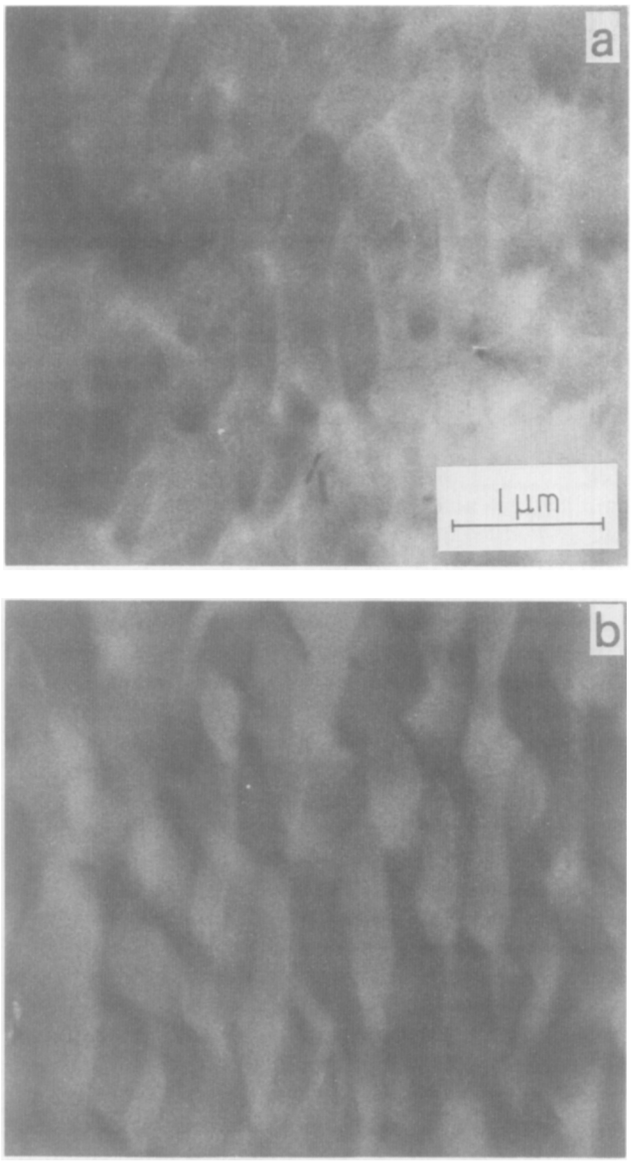

Figure 5 Micrographs of the same area of a specimen annealed for 5 s at 300°C; the shear direction is vertical. (a) Bright field showing domains separated by walls of light contrast. (b) E[W] dark field showing contrast associated with different chain orientations within the domains

pendicular to the shear direction are, as in *Figure 6*, not apparent in bright field, and must therefore be associated with a scheme of molecular reorientation which does not involve substantial changes in inclination to the specimen plane. Equivalent changes in contrast can also be seen in *Figure 7b* as, unlike *Figure 6b*, it is imaged in the 'wing' of the IM position. In addition some bright field images show that, for the fully developed domain structure, the orientation is not completely constant within any one domain, but that the out of plane tilt increases gradually towards the walls; this manifests itself as a slight darkening of domain contrast on moving from centre to edge.

The orientation of the walls with respect to the specimen plane is also a significant parameter. For grain boundaries in metals, tilting of the foil causes changes in the projected width of the planar feature; and from measuring the width of the boundary image as a function of tilt angle it is a matter of simple geometry to extract the inclination of the boundary plane to the specimen plane. This method works when a given planar feature (fixed in the specimen) remains in contrast for all inclinations. The case of the walls under investigation here is quite different. The image of the wall is centred where the molecules are most nearly parallel to the electron beam. As the specimen is tilted the apparent centre of the wall will move in the specimen. This shift in wall position upon tilting can be followed by using undissolved rocksalt remaining on the film surface as a marker. *Figure 8* shows the apparent movement of veins relative to surface rocksalt crystals as the specimen is tilted about an axis perpendicular to the shear direction; tilting in opposite senses about the flat position causes the veins to move in opposite senses also, and simultaneously alternate domains darken as they become oriented for greater scattering[12]. If the axis of tilt is instead parallel to the shear direction, significant changes in vein contrast occur (*Figure 9*) (different parts of the walls appear darker or lighter than when flat) but the domains themselves do not exhibit large contrast changes since their molecular orientation lies close to the shear direction. However, measurements of changes in position of the veins is less easy than from *Figure 8* because of the

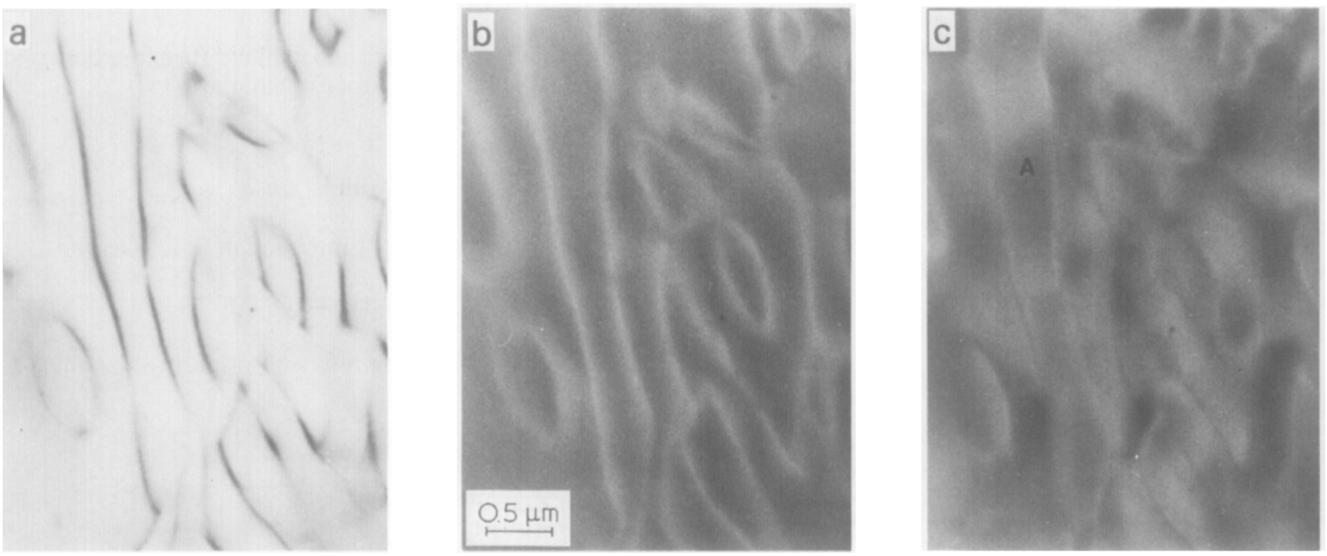

Figure 6 Micrographs of the same area of a sample annealed for 10 mins at 300°C. The shear direction is vertical. (a) Bright field showing dark veins. (b) IM dark field, the veins appear light. (c) E[W] dark field (the letter on the micrograph is referred to in the text)

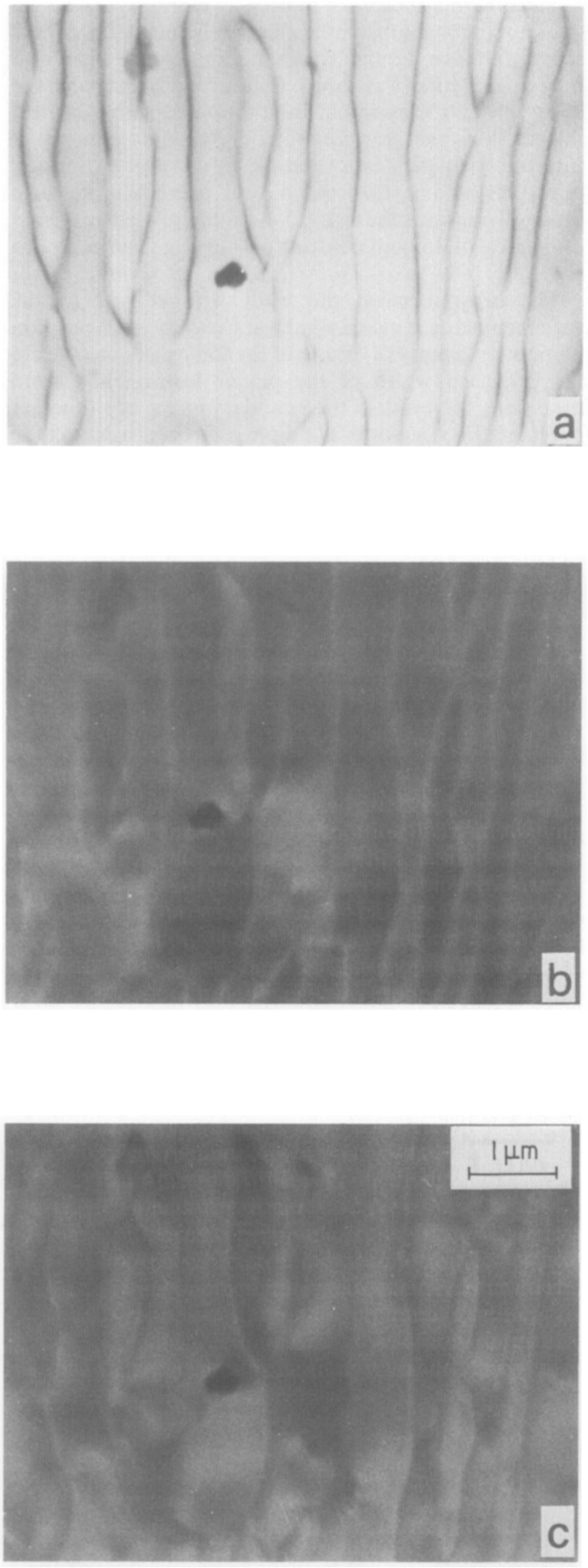

Figure 7 Micrographs of a different specimen but annealed under the same conditions as that of *Figure 6*. (a) Bright field. (b) IM[W] dark field. (c) E[W] dark field

foreshortening of distances perpendicular to the shear direction.

CALCULATION OF BRIGHT FIELD INTENSITY AS A FUNCTION OF MOLECULAR INCLINATION

It has previously been stated[12,16] that as the angle subtended by the molecular long axis to the electron beam decreases, the scattered intensity increases. For semi-crystalline polymers such as polyethylene, a similar effect has long been recognized[19,20] when increased excitation of a particular, discrete, set of reflections is involved. For LCP's true Bragg reflections are not present, and the problem must be considered in terms of the increased excitation of a diffuse equatorial ring. In this section a simplified calculation of the length of arc of the equatorial ring excited for a given molecular inclination will be set down, so that some measure of the degree of homoeotropy present in the boundary can be obtained.

For a crystalline material, whether a given reflection is significantly excited or not depends on the magnitude of the deviation parameter which describes the deviation of a reciprocal lattice point from the Ewald sphere (for a general discussion see ref. 21). Since the wavelength of 100 KeV electrons is small (0.037 Å), the Ewald sphere can be assumed to be a plane. Also, for this calculation the equatorial ring will be taken to be a cylinder of radius $s=1.4$ Å^{-1}, length $h=\pi s/9$ Å^{-1} (obtained from micro-diffraction experiments[22]) and zero thickness. The problem of determining the extent of the equatorial ring which is excited therefore reduces to a calculation of the length of arc representing the intersection of a plane with the cylinder described above; this will be approached by considering the cylinder to be fixed and the plane rotated.

Using the geometry of *Figure 10*, the cylinder can be represented parametrically by $(s\cos\xi,\ s\sin\xi,\ z)$ where $0<\xi<2\pi$ and $|z|\leqslant h/2$. Coordinates are chosen so that the x axis lies in the plane and θ is defined to be the angle between the normal to the plane and the y axis. For general rotations θ about the x axis the equation of the plane is

$$y\cos\theta - z\sin\theta = 0 \tag{1}$$

Intersection of the plane and cylinder therefore occurs at points which obey equation (1) and also

$$x^2+y^2=s^2 \quad \text{with } |z|\leqslant h/2 \tag{2}$$

An element of the arc of intersection dl is given by

$$dl^2 = dx^2+dy^2+dz^2,$$

and therefore differentiating with respect to the angle ξ, gives

$$\left(\frac{dl}{d\xi}\right)^2=\left(\frac{dx}{d\xi}\right)^2+\left(\frac{dy}{d\xi}\right)^2+\left(\frac{dz}{d\xi}\right)^2 \tag{3}$$

From equations (1) and (2)

$$z = y\cot\theta = s\sin\xi\cot\theta$$

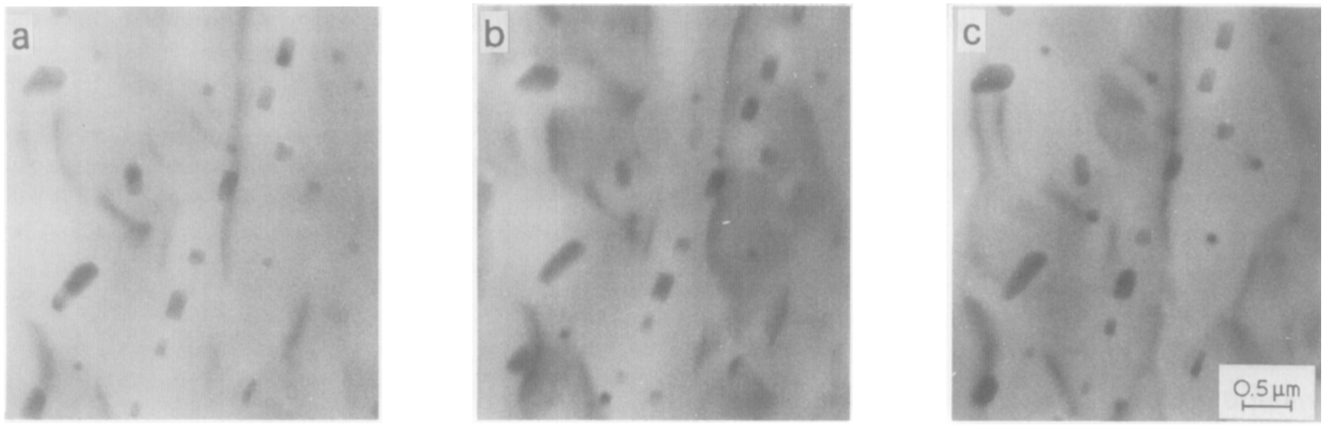

Figure 8 Micrographs showing changes in apparent position of veins in relation to rock salt crystals, on tilting the specimen about the horizontal axis (shear direction vertical). (a) 0°, (b) −24°, (c) +24°

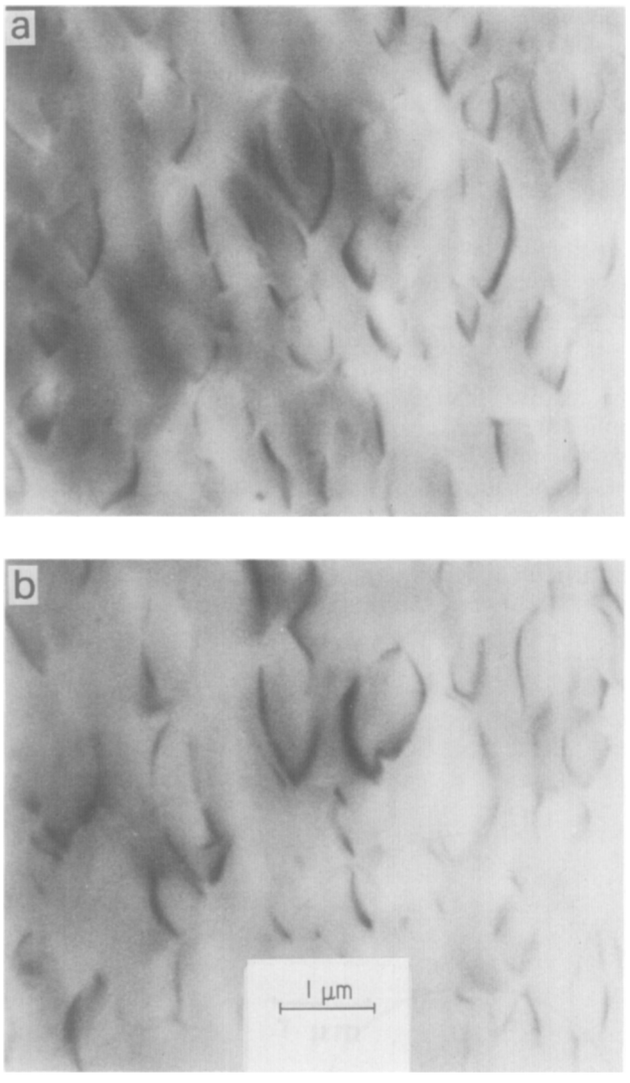

Figure 9 Changes in bright field contrast associated with a tilt about the vertical axis (also the shear direction)

and hence

$$|s \sin \xi \cot \theta| \leqslant h/2$$

to give

$$\xi_{max} = \sin^{-1}(h/(2s \cot \theta))$$

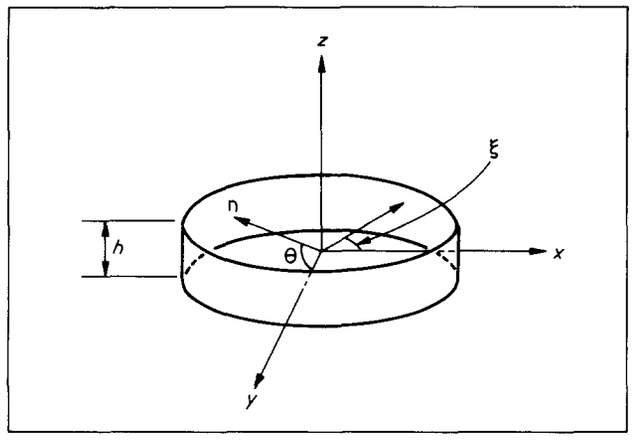

Figure 10 Parameters used to define the cylindrical surface (radius s, height h) in reciprocal space

and the total arc length l is obtained by substitution into equation (3) and subsequent integration to give:

$$l(\theta) = 2 \int_0^{\sin^{-1}(h/(2s\cot\theta))} (s^2 + s^2 \cot^2\theta \cos^2\xi)^{\frac{1}{2}} \, d\xi$$

This can be rewritten in terms of tabulated Elliptic integrals of the second kind, $E(\phi,\alpha)$[30],

$$l(\theta) = 2s\left(1 + \frac{h^2}{4s \sin^2\phi}\right)^{\frac{1}{2}} \int_0^{\phi} (1 - \sin^2\alpha \sin^2\xi)^{\frac{1}{2}} \, d\xi$$

$$= 2s\left(1 + \frac{h^2}{4s^2 \sin^2\phi}\right)^{\frac{1}{2}} E(\phi,\alpha) \qquad (4)$$

where

$$\sin\phi = h/(2s \cot\theta)$$

and

$$\sin^2\alpha = \frac{\cot^2\theta}{1 + \cot^2\theta} = \frac{1}{\frac{4s^2 \sin^2\phi}{h^2} + 1}$$

Taking values for h and s as given above, equation (4) can be plotted; the result is shown in *Figure 11*. In the limiting

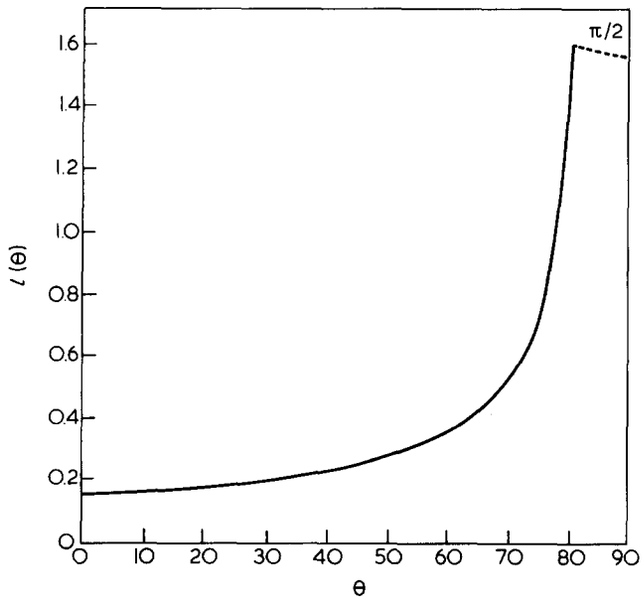

Figure 11 Plot of equation (4) showing the relationship between the length of the intersection of the cylinder, representing the distribution of intensity in reciprocal space, with the reflecting plane, and the angle between the chain axis and the specimen plane. The broken line represents the function given by equation (5)

case of $\theta=0$, the expression tends to $l(\theta=0)=h$ as expected (this implies the molecules are confined to the plane perpendicular to the electron beam). For $\theta \geqslant((\pi/2)-(h/2s))$ (i.e. $\xi>\xi_{max}$) equation (4) must be modified. At $\theta_{max}=\cot^{-1}(h/(2s\sin\xi))$, the arc length is a maximum (the ring is a complete ellipse); as θ increases further to $\pi/2$ the eccentricity of the ellipse decreases until it is a full circle at $\theta=\pi/2$, with $l(\pi/2)=2\pi s$. For this range of θ, $(\pi/2-h/2s)\leqslant\theta\leqslant\pi/2$, $\phi=\pi/2$ and $\sin^2\alpha=1/(\tan^2\theta+1)$.

Hence equation (4) is replaced by

$$l(\theta)=2s\left(1+\frac{h^2}{4s^2}\right)^{\frac{1}{2}}E\left(\frac{\pi}{2},\alpha\right) \qquad (5)$$

This is plotted in *Figure 11* as a broken line. The use of the curve for $l(\theta)$ for interpreting *TEM* images will be discussed below.

STEREOGRAPHIC REPRESENTATION OF MOLECULAR ORIENTATION AND ASSOCIATED CONTRAST

Given the form of *Figure 11*, it is possible to assess whether a given orientation of molecules will appear black, white or of intermediate contrast for any particular position of an objective aperture of given acceptance angle γ. Thus the loci of orientations which will appear as dark (or light lines) for bright and dark field images can be found, and these are most conveniently represented on a stereogram. The axes will be chosen such that the homeotropic orientation lies at the centre of the stereogram, and hence homogeneous orientations will lie on the circumference. The point representing the prior shear direction will be chosen to lie at the north (or equivalently south) pole. As with earlier figures, full circles will be used to denote orientations above the plane of the stereogram, and open circles those below, but antipodal points are physically equivalent in this system, since the molecules are non-polar ($+\underline{n}=-\underline{n}$).

For the experiments performed here, the acceptance angle of the objective aperture is equal to 1.2 radians. Reference to *Figure 12* shows that, for molecules which subtend an angle of β to the shear direction in the plane of the specimen, an aperture placed in the 'E' position will receive no intensity when

$$\frac{l}{2}+\frac{\gamma}{2}\leqslant\frac{\pi}{2}-\beta$$

and hence

$$\frac{l}{2}\leqslant 0.97-\beta \qquad (6)$$

Equation (6) and *Figure 11* give the limits of orientation (β,θ) for which the E dark field is black. They are plotted stereographically in *Figure 13* where they appear as equatorial lobes containing those orientations which will produce blackness. Also plotted are equivalent lobes (centred on top and bottom of the stereogram) which define the chain orientations which give blackness for the IM aperture position. Similar curves could be drawn for any position of the aperture (e.g. E[W] etc.). Curves for 'grey levels' in the dark field images can similarly be calculated.

To obtain the limiting curve of orientations which yield dark contrast in bright field images requires knowledge or the relative changes in scattering intensity which are sufficient to make a region look black relative to its surroundings. The experimental value of this change can be obtained from microdensitometry of the electron image plate and hence, using certain simplifying assumptions, the corresponding locus of orientations can be plotted on the stereogram. In general, for an electron beam traversing an amorphous specimen (i.e. a specimen

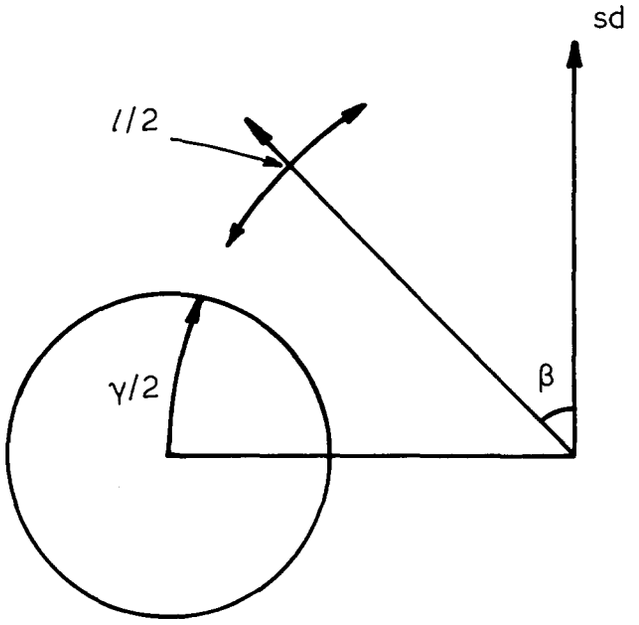

Figure 12 Diagram representing the relationship between aperture radius $\gamma/2$, arc length of equatorial maximum, $l/2$, and the misorientation angle β

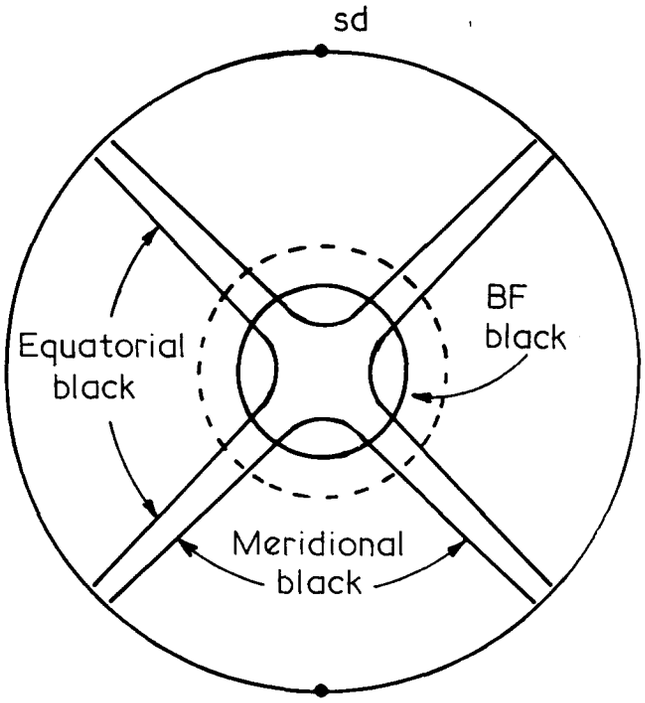

Figure 13 Stereographic plot of chain orientations which will give 'dark' contrast for the three different imaging modes used. The electron beam is normal to the specimen plane and corresponds to the central point, while the shear direction (sd) is marked at the top and bottom of the stereogram. Chain orientations within the equatorial lobes will give dark contrast for 'E' imaging. The lobes centred on the meridian contain chain orientations which will give dark contrast for the aperture at the IM position. For bright field, dark contrast occurs when the chains are tilted out of the specimen plane. The darkness thus increases towards the centre of the stereogram and this trend is represented by two concentric circular contours; the outer corresponding to a contrast level of 1.4, and the inner, a level of 2

for which Bragg reflections are unimportant, unlike a crystal) of thickness t, the optical density Φ of the electron image plate is of the form

$$\Phi = A I_0 \exp -t/\lambda \tag{7}$$

where I_0 is the incident beam intensity, A is a constant and λ is the effective mean free path for scattering. Microdensitometry combined with this equation has previously been used to measure changes in mass thickness due to crazes and deformation zones in glassy polymers (see e.g. refs. 23 and 24). However, for specimens where t is constant, but the effective mean free path for electrons is altered as the molecular orientation changes, the same approach may be used to extract relative values for λ in different part of a specimen, (λ_v, λ_D being the values in a vein and domain respectively).

Measurements of the optical density at a vein, Φ_v, the centre of a domain Φ_D and a hole Φ_h are made; and thus from equation (7):

$$\ln\left(\frac{\Phi_v}{\Phi_h}\right) = \frac{-t}{\lambda_v}$$

and,

$$\ln\left(\frac{\Phi_D}{\Phi_h}\right) = \frac{-t}{\lambda_D}$$

hence,

$$\frac{\lambda_D}{\lambda_v} = \frac{\ln(\Phi_v/\Phi_h)}{\ln(\Phi_D/\Phi_h)} \tag{8}$$

The ratio λ_D/λ_v obtained experimentally using equation (8) is approximately 1.4. Without knowledge of the out-of-plane tilt angle at the centre of the domain, this is of itself not sufficient to evaluate λ_D and hence the tilt of the molecules in a wall. However, a first order approximation can be made by assuming the molecules still lie in the specimen plane at the centre of the domains, to yield a value for the tilt in the wall of $\sim 45°$; this is clearly a lower bound. This analysis does demonstrate, however, that contrast changes as large as observed do not necessitate true homeotropy to be present anywhere.

In bright field therefore, the closer the molecular orientation is to the centre of the stereogram the darker the contrast. The locus of orientation which will give the observed contrast of 1.4 is thus a circle of angular radius 45° about the centre of the stereogram. This circle, together with that for a contrast of 2.0, is shown in *Figure 13*. From the curves shown on this Figure (and others appropriate to particular positions of the objective aperture) correlations of contrast in trios of micrographs such as *Figures 6* and *7* can be used to evaluate the orientation changes across a Bloch wall.

DISCUSSION

Straightforward schemes for the change in molecular orientation within walls have been described in the section dealing with possible wall geometries in LCP's, the contrast changes observed in the *TEM* in the Results section, and the specific relationships between molecular orientation and contrast are embodied in *Figure 13*. It is now possible to determine which of the simpler possible orientation routes are compatible with the observed contrast at the walls.

Bright field tilting experiments show that domains with an in-plane misorientation to one side of the shear direction tend to be inclined out of the specimen plane in one sense, while those misoriented to the other side are inclined in the other sense. This orientation coupling has already been described and discussed[12]. Adjacent domains in these two different orientations, as plotted in *Figure 14a*, will form the initial framework for discussing the structure within the walls themselves.

Walls showing light contrast after short anneals

Walls such as those in *Figure 5a*, which appear light in bright field, suggest immediately that whereas opposite tilts out of the specimen plane have formed in the adjacent domains, the rotation of the molecular director on traversing the wall passes through the in-plane or homogeneous orientation. *Figure 14b* shows that for a wall containing the shear direction (i.e. appearing parallel to it on the micrograph), the plane of the wall can be oriented to contain both directors thus ensuring a pure twist wall. The reorientation route drawn passes through the homogeneous (planar) orientation and can account for the observed contrast. Other wall orientations which contain the shear direction, but not the domain directors, will require both the bend and twist distortions associated

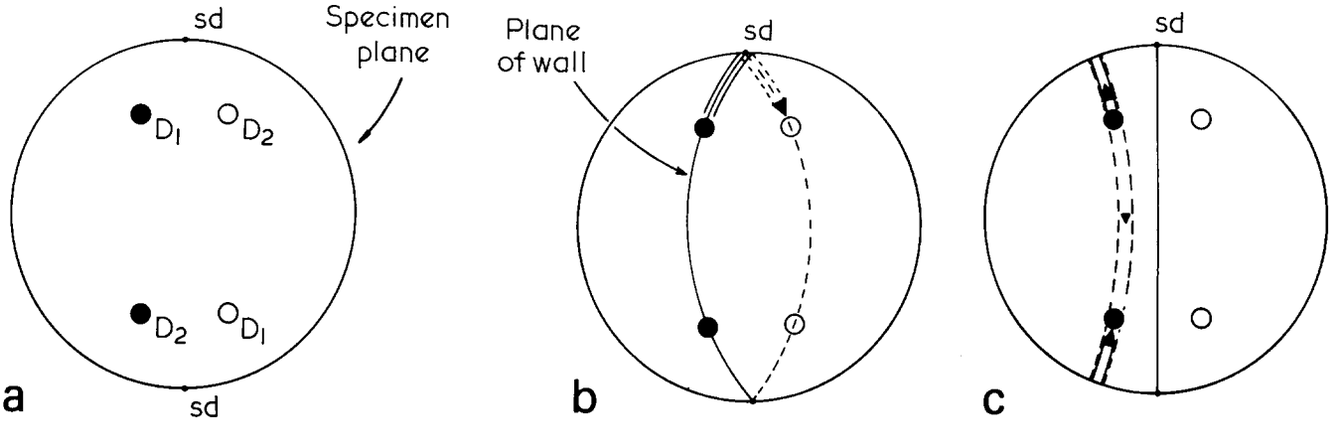

Figure 14 (a) Stereogram of chain orientations in adjacent domains in relation to the plane of the specimen (the circumference) and the shear direction (sd). (b) Stereogram showing the plane of the wall and the reorientation route within the wall (double arrow) which involves only twist distortion compatible with the micrographs of *Figure 5* for specimens annealed for 5 s at 300°C. (c) Another possible reorientation route which would give light contrast in bright field (albeit twice) and involve bend as well as twist distortions

with the small circle reorientation route. Such a route, for a wall oriented perpendicular to the specimen plane (i.e. of minimum area), has been drawn in *Figure 2b*. It will only pass through the homogeneous orientations, consistent with the observed light contrast (*Figure 5a*), if it follows the long route around the small circle as drawn in *Figure 14c*. However, this route would predict double light boundaries which are not seen. For the preferred wall alignment along the shear direction, the experimental evidence thus supports the wall orientation and great circle, twist-only reorientation route depicted in *Figure 14b*.

It is not clear for LCP's which of bend or twist distortions has the lower energy. Limited experimental data on lyotropic systems[18] suggests that K_{33} (bend) may be less than K_{22} (twist) while K_{11} (splay) is much greater than either: but Kléman *et al.*[25] suggest that for a particular thermotropic polymer K_{22} is definitely lower than K_{33}. However, for the walls under consideration here, the total angular distortion must be considered as well as the relative magnitudes of the elastic constants. Of the reorientation routes which pass through the specimen plane, the great circle, twist-only, route is the most direct and hence possesses the smallest total angular reorientation leading to a reduction in the energy of distortion involved. It therefore seems likely that the twist only route will be favoured, as indicated by experiment. In this case, it is easy to explain the observed elongation of domains in the shear direction, for only walls containing this direction have the option of having a pure twist configuration.

Walls appearing dark in bright field (veins)

After longer annealing times, at least for this particular copolyester, boundaries which initially appeared light in bright field are apparent as dark veins. The veins cannot simply be attributed to a sharp, local change in thickness. This statement is supported both by the way the position of the veins moves upon specimen tilting (*Figure 8*), and by their appearance after shadowing. An annealed specimen was lightly shadowed with gold-palladium at a shallow angle, perpendicular to the shear direction, so that the underlying veins were still clearly visible by diffraction contrast. *Figure 15* shows a typical area, which demonstrates that no surface ridge is associated with the veins.

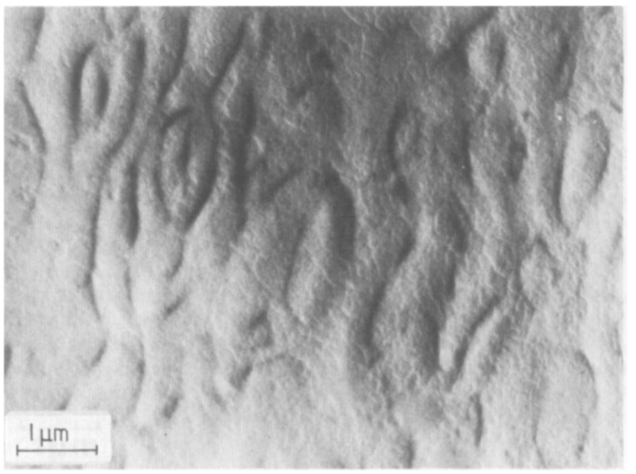

Figure 15 Lightly shadowed specimen containing veins as seen in bright field. The veins are still apparent through the coating, yet there is no distinct surface relief associated with them

The marked change in contrast as the veins form is associated with a total change in reorientation route across the walls: for the molecules now pass closer to homeotropy within the wall. In these specimens, the majority of walls can be seen to lie parallel to the shear direction and this orientation of wall will be considered first. As with the light contrast walls already discussed, there are two particular options for a wall configuration which would give dark vein contrast. One is a 'twist only' great circle route, while the other, which permits the boundary to lie perpendicular to the specimen plane and thus minimize its area, follows a small circle route and therefore involves both twist and bend distortions. The two possibilities are shown in *Figures 16a* and *16b*.

Unlike the light contrast case, the reorientation route lengths are comparable and the issue as to which is actually followed rests on the balance between the reduction in boundary area, and hence energy, and the consequent introduction of bend as well as twist distortion. However, it is possible, through close examination of dark field images in conjunction with *Figure 13*, to distinguish between routes I and II.

Figures 17(*a*), (*b*) and (*c*) show the images of walls in the three imaging modes and *Figures 17*(*a'*), (*b'*) and (*c'*) show

the corresponding loci of dark contrast associated with these three modes. In all three pairs, the contrast is consistent with route II of *Figure 16* which is also marked on *Figures 17a', b'* and *c'*. In the E[W] image, the thin dark line at the wall corresponds to the orientational route intersecting the 'nose' of the dark contrast region. In this case the boundary appears much narrower than in either the bright field or IM dark field images, because only the centre of the wall gives rise to the dark contrast, rather than the majority of the boundary width as in bright field. *Figure 17* therefore confirms the association of the vein type boundaries with the near homeotropic small circle route (II).

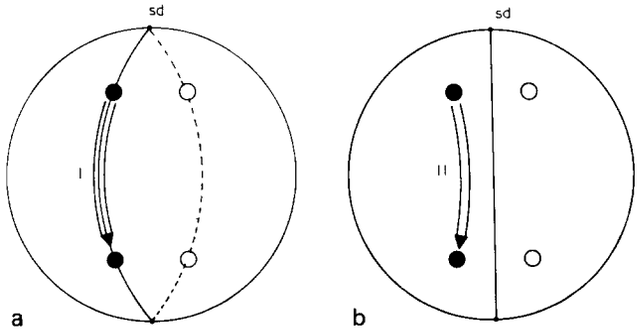

Figure 16 Stereogram of two reorientation routes. (a) A route (I), which involves only twist distortion and requires the wall to contain the two domain orientations. (b) A small circle route (II), involving both twist and bend distortions, which enables the wall to lie perpendicular to the specimen plane

It is clear that walls involving near homeotropic orientation must require segregation of molecules not much longer than the specimen is thick. Such segregation will be rate controlling in the formation of such walls, which explains why they only appear after longer anneals whereas, at 300°C, the domain structure itself forms almost immediately. These processes have been fully described in the previous paper[12].

Walls with little contrast in bright field

In the developed domain structure containing veins, walls which lie nearly perpendicular to the shear direction tend to show little or no contrast in bright field. However, E[W] dark field contrast reveals their presence through the associated molecular re-orientation. The only possible route for a boundary normal to the shear direction separating domains with opposite senses of in-plane misorientation and out-of-plane tilt is shown in *Figure 18a*. It is long, and would pass through planar orientation producing a light and dark contrast sequence which is not observed. Instead, it appears that these boundaries separate domains which, although possessing opposite misorientations in the specimen plane, are inclined out of the plane in the same sense. The small circle route on the corresponding stereogram is shown in *Figure 18b*. Comparison with *Figure 13* explains the general lack of bright

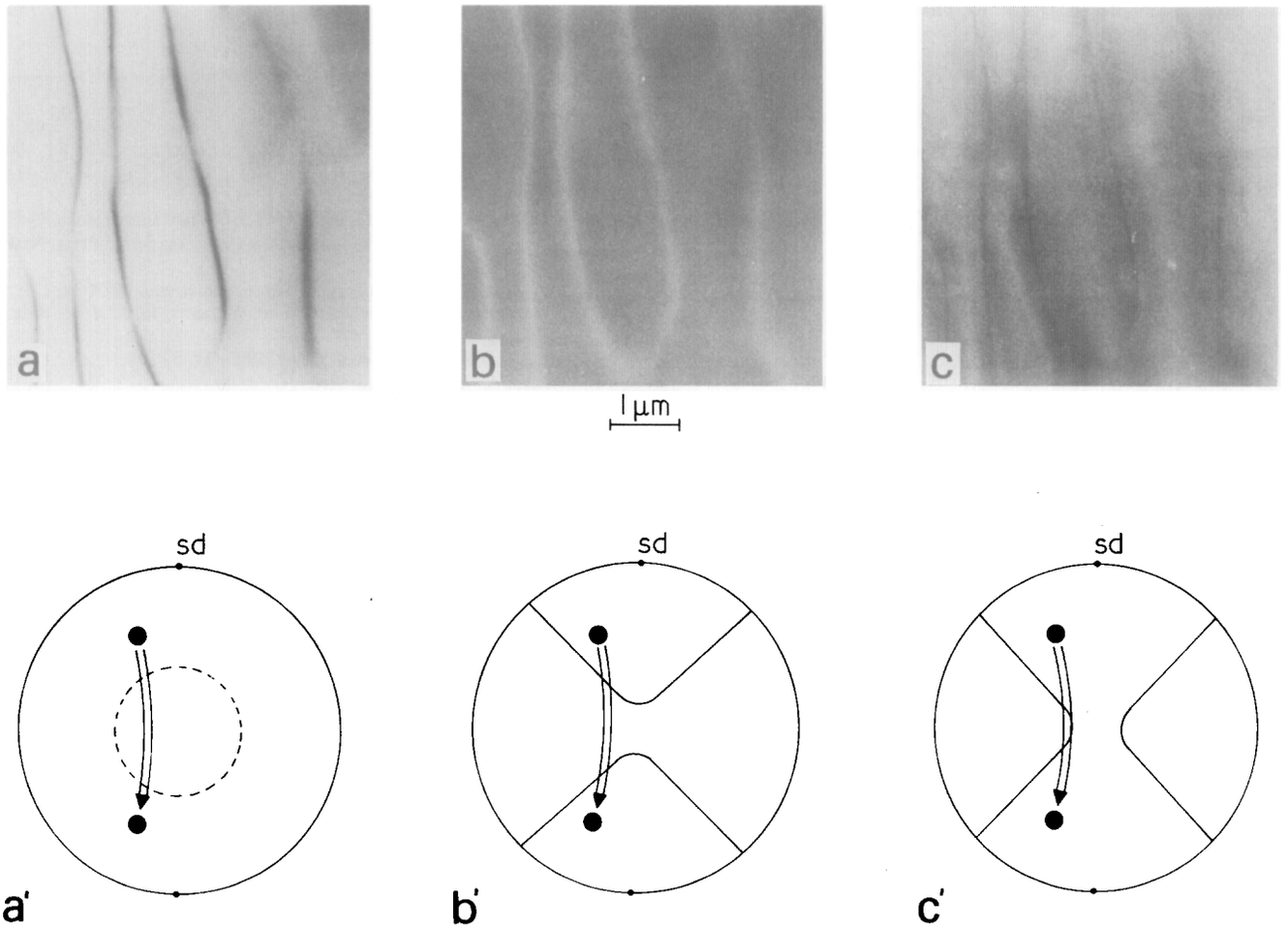

Figure 17 (a), (b) and (c) are images of the walls in bright field, dark field IM and E respectively. The shear direction is vertical. Stereograms (a'), (b') and (c') are the corresponding plots of the loci of dark contrast for the three modes. The reorientation route II of *Figure 16(b)* is plotted on the three stereograms and it is seen to be compatible with the contrast changes of the three micrographs. In particular the thin dark veins in the image (*Figure 17(c)*) distinguish this route from the great circle possibility, route I of *Figure 16(a)*, which would lead to wider dark veins

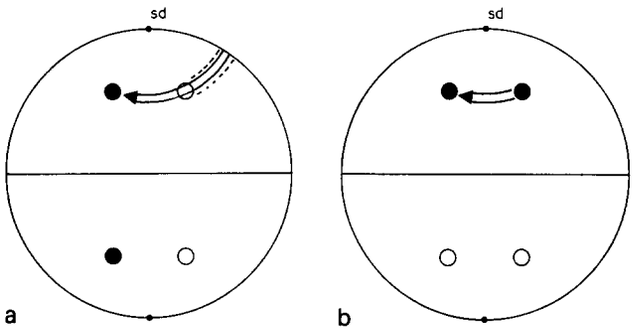

Figure 18 Stereograms showing possible reorientation routes for boundaries normal to the shear direction which do not appear as dark veins in bright field. *Figure 18a* is drawn for the domain orientations previously considered, whereas *Figure 18b* is based on adjacent domains which are tilted out of the specimen plane in the same sense

field contrast (in fact such boundaries sometimes appear faintly dark). The wall is visible in E[W] dark field as the demarcation between differing contrast levels in adjacent domains.

CONCLUSIONS

This paper has focussed attention on the walls in LCP's which separate domains of different molecular orientation. The domains develop when thin specimens of a thermotropic copolyester showing the banded texture are annealed above their softening point. The chains within each domain lie more or less parallel, but the misorientation between domains is typically a few tens of degrees. The nature of the orientation distribution of the domains and its developement with increased annealing time has already been discussed[12]. The particular copolyester which was the subject of this detailed study had a comparatively low intrinsic viscosity (*IV*) and showed the development of vein type walls after longer annealing times.

The low concentration of chain ends in liquid crystal polymers means that splay distortions involve a high energy penalty and are thus unlikely. It is therefore necessary that the chain flux within the wall and normal to its plane must be the same as in the domains which it separates. This condition limits the possible orientations of a wall to those which contain one or other of the bisectors between the chain long axes in the adjacent domains; it also limits the chain reorientation within a wall, as a constant angle to the wall normal must be maintained. Walls which lie parallel to the chain orientations in each of the adjacent domains will involve only twist distortions, while the general case (for constant flux) necessitates both bend and twist distortion.

There is a strong tendency for the domains to be elongated along the original shear direction, and the majority of the walls are parallel to this direction. At 300°C the banded structure transforms to a domain structure within a few seconds, and after 5 s, chains in adjacent domains have tilted out of the specimen plane in opposite senses, while within the wall the reorientation route still passes through the specimen plane. The walls parallel to the shear direction in lightly annealed specimens are oriented so that they contain the chain directions of both domains and are not necessarily perpendicular to the specimen plane. They contain only twist distortions.

After longer anneals the walls undergo a marked change in appearance and develop dark contrast in bright field. Consideration of the relationship between chain orientation and contrast in the bright field and dark field equatorial and meridional imaging modes, has demonstrated that the reorientation route within the wall tilts the chains further out of the specimen plane, so that they pass through an orientation close to the specimen normal (the homeotropic orientation) before rotating back towards the specimen plane. The observation of fine dark band contrast in equatorial dark field suggests that the walls are now approximately normal to the specimen plane and that they contain both twist and bend distortions. The development of walls in which the chains rotate through near homeotropic orientations is probably controlled by the segregation of lower molecular fractions. Such walls readily form only in samples with molecular weight distributions corresponding to relatively low *IV*s[12].

ACKNOWLEDGEMENTS

Thanks are due to the SERC for financial support (through a grant and a fellowship), to Professor R. W. K. Honecombe FRS for the provision of laboratory facilities and Drs Griffin and Ryan of ICI (Plastics and Petrochemicals Division) for providing both the polymer and measuring its *IV*. Useful discussions with Dr M. J. Donald are gratefully acknowledged.

REFERENCES

1 Chandrasekhar, S. 'Liquid Crystals', Cambridge University Press, 1977
2 Nehring, J. and Saupe, A. *J. Chem. Soc. Faraday Trans.* 1972, **68**, 1
3 Ryschenkow, G. and Kleman, M. *J. Chem. Phys.* 1976, **64**, 404
4 Demus, D. and Richter, L. 'Textures in Liquid Crystals', Verlag Chemie, Weinheim, New York, 1978
5 Kleman, M. 'Points, Lines and Walls', Wiley Interscience, 1983
6 Meyer, R. B. in 'Polymer Liquid Crystals', Academic Press, New York, 1982, Ch. 6
7 de Gennes, P. G. *Mol. Cryst. Liq. Cryst. (Lett.)* 1977, **34**, 177
8 Meyerhofer, D., Sussman, A. and Williams, R. *J. Appl. Phys.* 1972, **43**, 3685
9 Leger, L. *Mol. Cryst. Liq. Cryst.* 1973, **24**, 33
10 Steib, A., Baur, G. and Meier, G. *J. de Phys.* 1975, **36**, Cl-185
11 Donald, A. M. and Windle, A. H. *J. Mater. Sci.* 1983, **18**, 1143
12 Donald, A. M. and Windle, A. H. *J. Mater. Sci.* 1984, **19**, 2085
13 Viney, C. and Windle, A. H. *J. Mater. Sci.* 1982, **17**, 2661
14 Viney, C., Mitchell, G. R. and Windle, A. H. *Polymer* 1983, **24** (*Commun.*), 145
15 Donald, A. M., Viney, C. and Windle, A. H. *Polymer* 1983, **24**, 155
16 Donald, A. M. *J. Mater. Sci. Lett.* 1984, **3**, 44
17 de Gennes, P. G. 'The Physics of Liquid Crystals', Oxford University Press, 1974
18 DuPre, D. private communication
19 Grubb, D. T. and Keller, A. *J. Mater. Sci.* 1972, **7**, 822
20 Grubb, D. T. *J. Mater. Sci.* 1974, **9**, 1715
21 Hirsch, P. B., Howie, A., Nicholson, R. B., Pashley, D. W. and Whelan, M. J. 'Electron Microscopy of Thin Crystals', Butterworths, London, 1965
22 Donald, A. M. and Windle, A. H. *Colloid Polym. Sci.* 1983, **261**, 793
23 Lauterwasser, B. D. and Kramer, E. J. *Phil. Mag.* 1979, **39A**, 479
24 Donald, A. M. and Kramer, E. J. *J. Mater. Sci.* 1981, **16**, 2977
25 Kléman, M., Liebert, L. and Strzelecki, L. *Polymer* 1983, **24**, 295
26 Millaud, B., Thierry, A. and Skoulios, A. *J. de Phys.* 1978, **39**, 1109
27 Noël, C., Billard, J., Bosio, L., Friedrich, C., Laupretre, F. and Strazielle, C. to be published
28 Mackley, M. R., Pinaud, F. and Siekmann, G. *Polymer* 1981, **22**, 437
29 Kléman, M. and Williams, C. *Phil. Mag.* 1973, **28**, 725
30 Handbook of Mathematical Functions, Eds. M. Abramowitz and I. A. Stegun, NBS Appl. Maths. Series **55** (1964)